

# Optimisation of Simulations of Stochastic Processes by Removal of Opposing Reactions

## Supplementary Information

Fabian Spill,<sup>1,2</sup> Philip K. Maini,<sup>3</sup> and Helen Byrne<sup>3</sup>

<sup>1</sup>*Department of Biomedical Engineering, Boston University, 44 Cummington Street, Boston MA 02215, USA*

<sup>2</sup>*Department of Mechanical Engineering, Massachusetts Institute of Technology, 77 Massachusetts Avenue, Cambridge, MA 02139, USA*

<sup>3</sup>*Wolfson Centre for Mathematical Biology, Mathematical Institute, University of Oxford, Oxford OX2 6GG, UK*

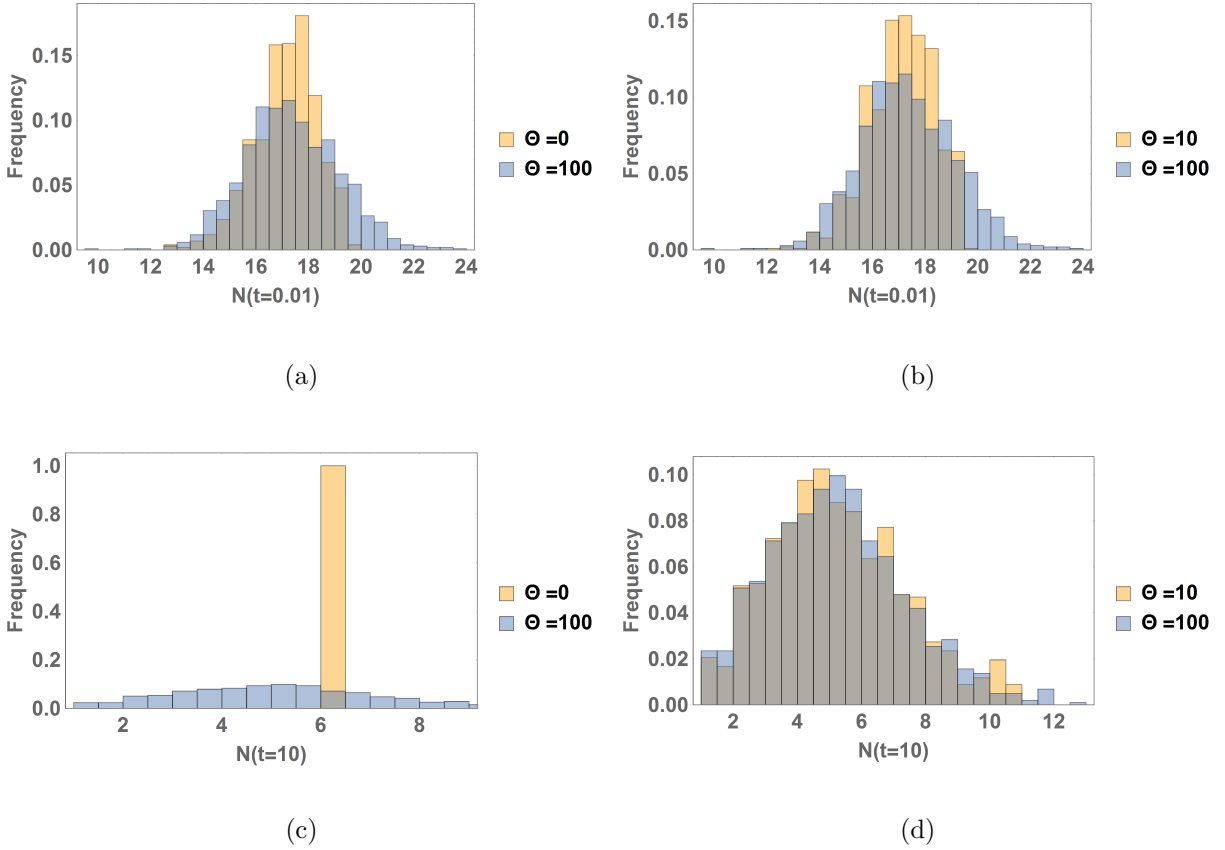
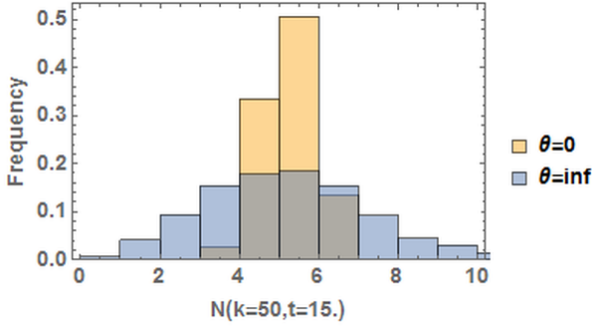
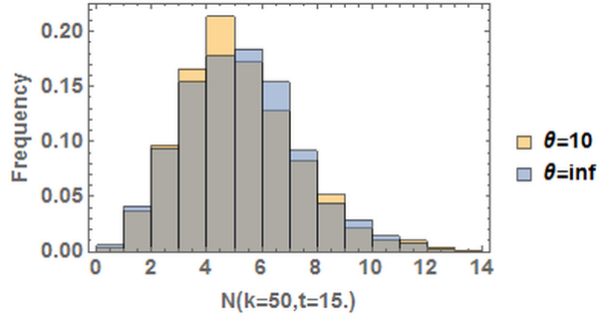


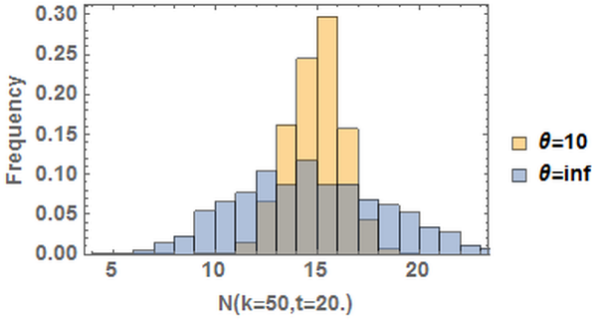
FIG. S1: Distribution of the birth-death process for the same parameters as in Figure 1, obtained from running 1024 different simulations, for two thresholds  $\Theta = 0, 10$ . In each case, we compare to the exact model, obtained by choosing a threshold  $\Theta = 100$ . The initial condition was  $N(t = 0) = 20$ , and the steady state is at  $N = 6$ . We notice that at  $t = 0.01$ , the distributions of all three cases,  $\Theta = 0, 10, 100$  are similar, but, by construction, for  $\Theta < 20$ , no birth can occur so the distribution is bounded by  $N(t = 0)$ . At  $t = 10$ , the distributions for  $\Theta = 10, 100$  look indistinguishable, whereas the distribution for  $\Theta = 0$  goes to the delta distribution, and the solution is trapped at the absorbing state.



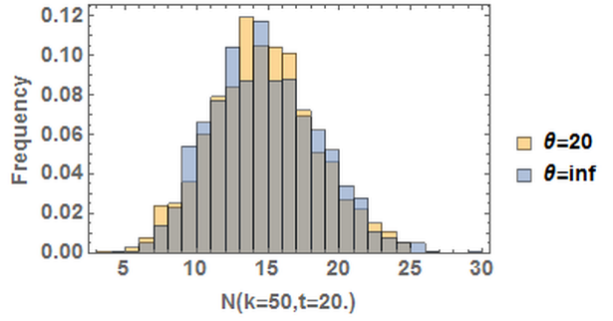
(a)



(b)



(c)



(d)

FIG. S2: Distribution of number of particles in compartment  $k = 50$  for the diffusion process described in section III A, where initially 1000 particles are seeded in the compartment on the left, with all other compartments empty. After  $t = 15$ , we see that, while the conditional difference model with a threshold of  $\Theta = 10$  closely matches the exact model ( $\Theta = inf$ ), panel (b), the model with a threshold of  $\Theta = 0$  shows a much narrower distribution than the exact model (panel (a)). At time  $t = 20$ , the case of  $\Theta = 10$  now also deviates visibly from the exact case (panel (c)), whereas the case of  $\Theta = 20$  offers close agreement (panel (d)).

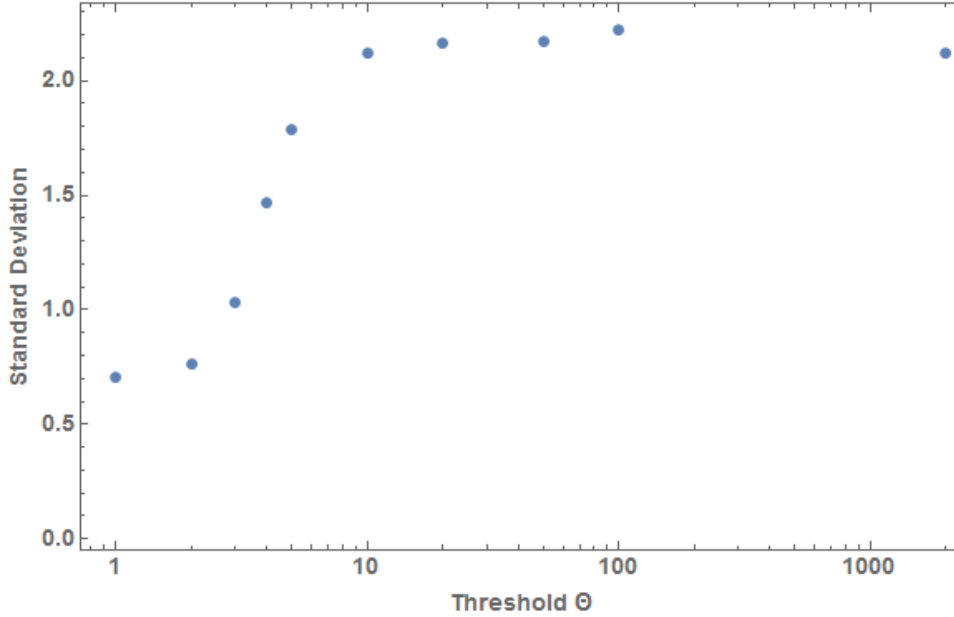


FIG. S3: Standard Deviation of the diffusion process described in section III A, obtained from distributions similar to those shown in Figure S2. Here, measurements are taken at fixed time  $t = 5$  in compartment  $k = 30$ , from 1024 simulations. We see that the standard deviations approach the ones of the exact model for thresholds around  $\Theta = 10$ .

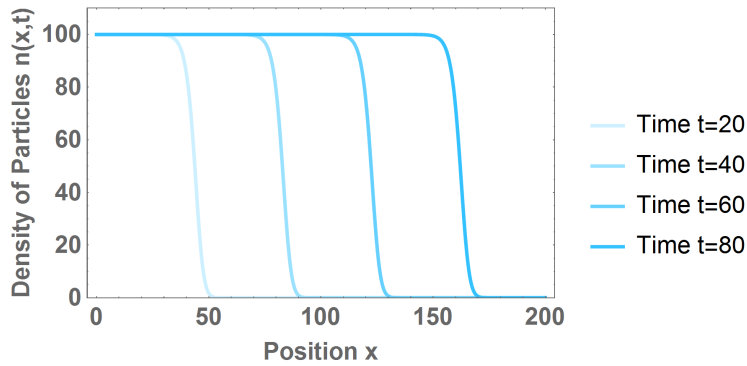


FIG. S4: Travelling waves of the deterministic Fisher-Kolmogorov equation for parameters  $D = 1$ ,  $\lambda = 1$  and  $\Omega = 100$ . We see that a traveling wave is spreading with constant velocity  $v = 2\sqrt{D\lambda} = 2$ .

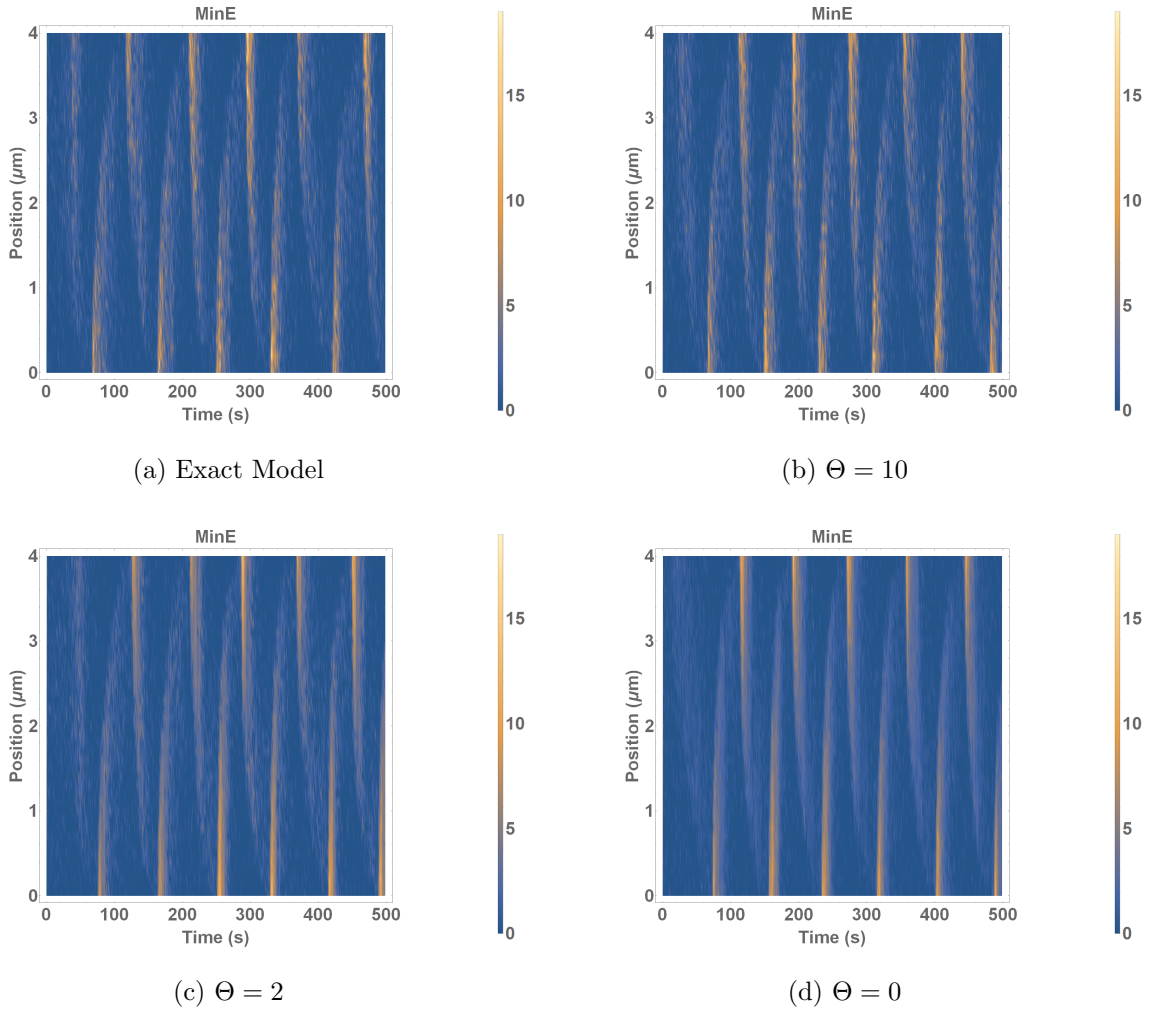
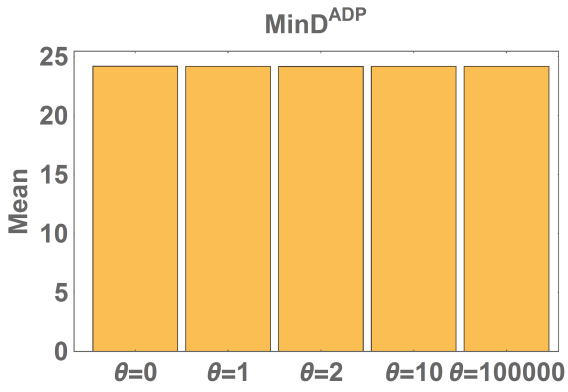
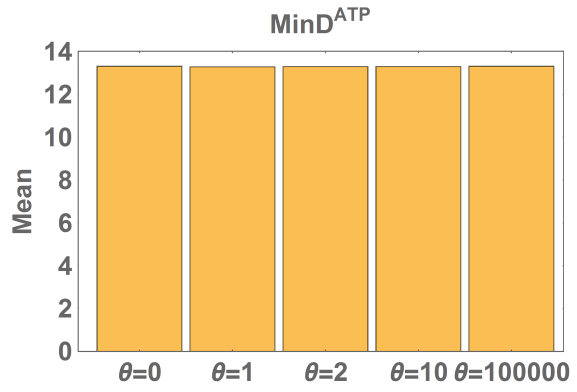


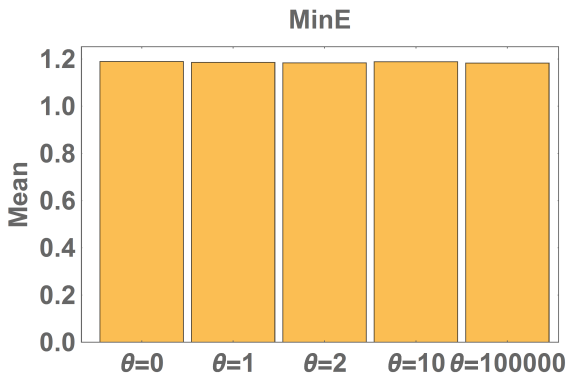
FIG. S5: Space-Time evolution of the number of MinE molecules with an initial number of 1400 MinE and 6700 MinD proteins. We compare simulations of the stochastic model where diffusion is modeled by the hybrid approach, equation (??), with different thresholds. Stable oscillations are forming after less than 100s. All four cases appear similar, but the cases with low thresholds,  $\Theta = 0, 2$ , appear less noisy than the case  $\Theta = 10$  and the case of normal diffusion.



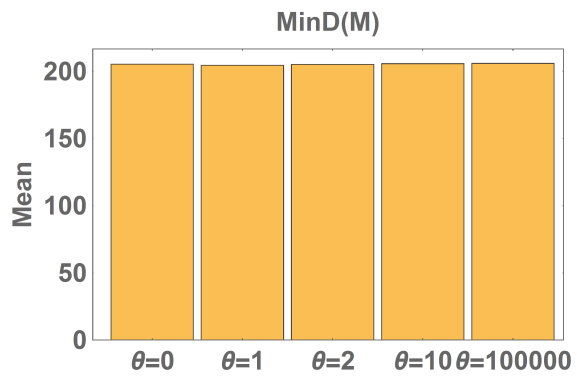
(a)



(b)

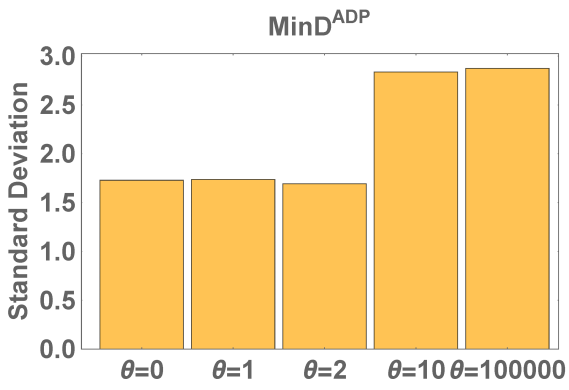


(c)

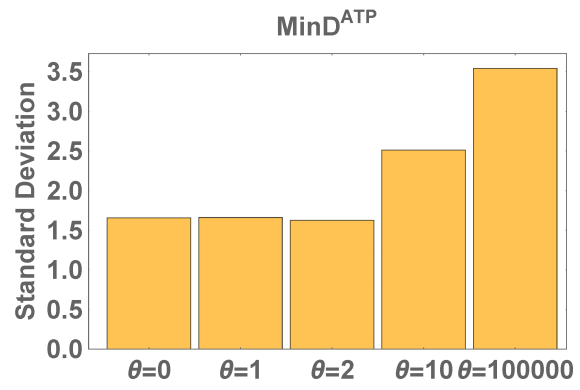


(d)

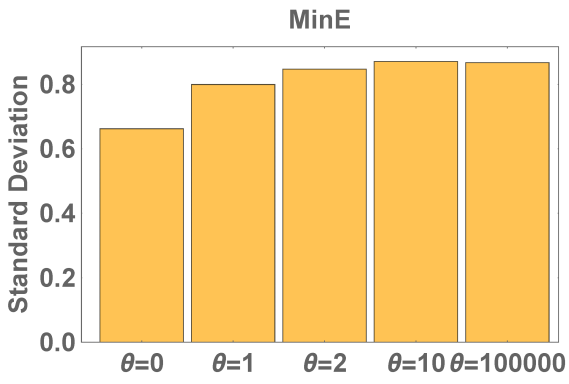
FIG. S6: Mean of the distributions shown in Figure 6, corresponding to the standard deviations shown in Figure 7.



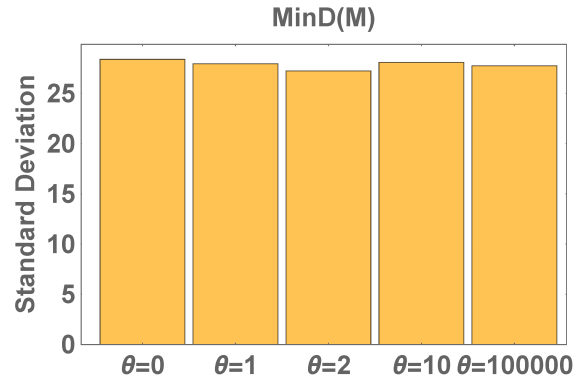
(a)



(b)



(c)



(d)

FIG. S7: Standard deviations from the distributions of particles, as in Figure 7, but for  $\frac{1}{4}$  of the number of particles.

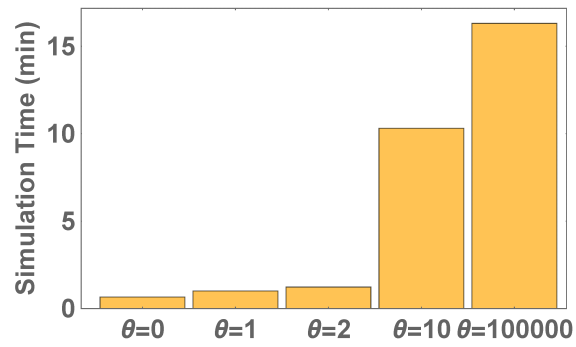


FIG. S8: Simulation performance as in Figure 8, but with only a quarter of the total number of particles.